Disturbance Rejection with Bounded Control Action: Loop-Shaping Methodology

Jose L. Figueroa, Osvaldo Agamennoni, and Jose A. Romagnoli
ICI Laboratory of Process System Engineering, Dept. of Chemical Engineering, The University of Sydney, Sydney, NSW, 2006, Australia

Suppressing the influence of external disturbances on a process is the most common objective of a controller in a chemical plant. A control system that can keep the controlled variables at or near their set point and the manipulated variables lower than their prespecified maximum bounds in the face of load disturbances is wanted. A method is presented to design controllers with disturbance rejection specifications and limits over the control energy. This methodology is based on a special strategy to shape the structured singular value of a closed-loop transfer function matrix.

Introduction

The main objective of any regulatory feedback control scheme is to keep the controlled outputs "close" to their desired value (or set points). What is meant by "close" can be defined in terms of various stability and performance requirements for the closed-loop system. However, some system characteristics make it difficult. One of these factors is the presence of disturbances in the process to be controlled (often called load changes). The suppression of the impact that disturbances have on the operating behavior of processing units is one of the main reasons for the use of control in the chemical industry.

Surprisingly, the issue of disturbance rejection has not been widely discussed in the general literature on controllability analysis. Of course, it has been known for a long time that disturbance rejection is an important property of the closed-loop system. This issue has been discussed in the context of controlling distillation columns (McCune and Gallier, 1973; Agamennoni et al., 1994) and lately some systematic tools for quantifying the effect of disturbances have been introduced (Skogestad and Wolff, 1992; Wolff et al., 1992).

The design of compensators to produce closed-loop systems with certain disturbance attenuation capabilities has been treated by Zames and Francis (1983), Francis and Zames (1984), and Chang and Pearson (1984) in terms of optimizing the sensitivity function. Since control energy is not penalized, the resulting controllers are usually improper for continuous time systems. Francis (1984) considers a more general situation, introducing a control energy in the cost function and solving the resulting problem using the H_∞ approach.

In this article, a methodology is presented to design controllers with disturbance rejection specifications and bounds over the control energy. This methodology is based on the use of a loop-shaping technique to adjust the structured singular values of the closed-loop system matrix to achieve a desired frequency response. This approach allows us to establish a general framework to the solution of the general disturbance rejection problem. The usefulness of this technique is discussed within the context of two examples, one of them an existing distillation column.

Disturbance Rejection Problem

Let us consider the closed-loop system of Figure 1a. Here $G(s)$ and $G_d(s)$ are transfer function matrices that describe the dynamic behavior between the vector of manipulated inputs $u'(s)$ and the vector of physical disturbances $d'(s)$ to the vector of controlled variables $y'(s)$, respectively. The linear feedback controller is denoted as $K'(s)$. The weighting functions W_u and W_y are introduced to perform an appropriate scale to u and y. This is an important aspect, since most of the disturbance rejection measures are scale dependent.

It is important first to describe how disturbances may deteriorate the behavior of the control system. Disturbances may affect a control loop either by:

(a) Introducing a large departure of the output value from the reference, or
(b) Affecting the output during a long period of time.

The relative importance of one or the other strongly depends

Correspondence concerning this article should be addressed to J. A. Romagnoli.
J. A. Romagnoli is the Joint ICI–University of Sydney Chair in Process Systems Engineering.

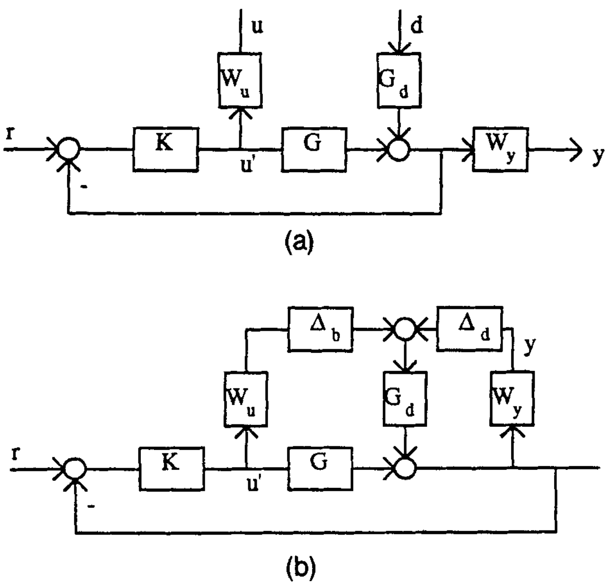

Figure 1. (a) Standard closed-loop system; (b) closed-loop with virtual uncertainty.

on the performance criteria. There are two aspects in this problem that need to be considered:

(1) The bandwidth of the disturbance transfer function (G_d).

(2) The disturbance signal characteristics (d).

In this article, we will focus our attention on disturbance signals frequently encountered in chemical plants, that is, steps, pulses, and ramps. The gain of G_d is not considered in our analysis because it is obvious that smaller values in the gain of G_d are always preferable.

Now, if G_d has a large bandwidth, disturbance signals with high-frequency components (pulses) will produce fast and large variations in the output from the reference value. In this sense, plants with smaller disturbance transfer function bandwidths are preferred (Skogestad and Wolff, 1992). However, if G_d has a small bandwidth, that is, sluggish poles, a low-frequency disturbance signal like a step will introduce smaller variations from the reference value, but it will last for a long period of time. This problem was considered by Agamennoni et al. (1994) in the context of designing a disturbance rejection controller for an industrial distillation column. Thus, it is not obvious *a priori* which plants are preferred since the decision will depend on three aspects:

(1) The objective to be achieved.

(2) The disturbance signal.

(3) The disturbance transfer function characteristics.

In the next section a loop-shaping technique will be described that allows us to solve the disturbance rejection problem under these general conditions. To this end, it is important first to study the inherent control limitations of these kinds of plants. It is instructive to study the special case of perfect control. From Figure 1a, the plant model is

$$y(s) = W_y(s)[G(s)u'(s) + G_d(s)d(s)], \tag{1}$$

then, for a square plant, perfect control ($y = r$) is achieved if we apply the following input signals

$$u(s) = W_u(s)^{-1}G(s)^{-1}\left[W_y(s)^{-1}r(s) - G_d(s)d(s)\right]. \tag{2}$$

From this equation it clearly follows that for load changes $[r(s) = 0]$ a bound on the amplitude of the manipulated variable u_j is needed to reject a disturbance d_k in all outputs and is given by

$$|u_j(s)| \le \sum_{k=1}^{n} |\delta_{jk}(s)||d_k(s)|, \tag{3}$$

where

$$\delta(s)_{jk} = \left[W_u(s)^{-1}G(s)^{-1}G_d(s)\right]_{jk} \tag{4}$$

and n is the number of system outputs.

The magnitude of δ_{jk} gives an interesting measure of the effect of each disturbance in the plant, that is, if the value of δ_{jk} is large, then a disturbance in the k-output has a large effect over the magnitude of the manipulated variable u_j.

From Figure 1a, the closed-loop transfer function between $d(s)$ and $y(s)$ is

$$y(s) = W_y(s)S(s)G_d(s)d(s), \tag{5}$$

and the transfer function between $d(s)$ and the weighted manipulated $u(s)$ variable is

$$u(s) = -W_u(s)K(s)S(s)G_d(s)d(s), \tag{6}$$

where, $L(s) = G(s)K(s)$ is the loop transfer function, $F(s) = I + L(s)$ is the return difference matrix, and $S(s) = [I + L(s)]^{-1}$ is the sensitivity matrix. In the following, the Laplace variable s or frequency argument $j\omega$ usually will be omitted to simplify notation.

Now, consider a disturbance d, with $\|d\|_2 = 1$, applied to the system. Then, from Eq. 5 and the singular value inequalities

$$\bar{\sigma}(AB) \le \bar{\sigma}(A)\bar{\sigma}(B)$$

and

$$\bar{\sigma}(AB) \le \underline{\sigma}(A)\bar{\sigma}(B)$$

we have

$$\bar{\sigma}\{W_yS\}\underline{\sigma}\{G_d\} \le \|y\|_2 \le \bar{\sigma}\{W_yS\}\bar{\sigma}\{G_d\}, \tag{7}$$

which gives

$$\|y\|_2 \le 1 \quad \text{if} \quad \frac{1}{\bar{\sigma}\{W_yS\}} \ge \bar{\sigma}\{G_d\} \tag{8}$$

and

$$\|y\|_2 \le 1 \quad \text{only if} \quad \frac{1}{\bar{\sigma}\{W_yS\}} \ge \underline{\sigma}\{G_d\}. \tag{9}$$

These are the conditions that the frequency response of the singular values of the sensitivity and the disturbance transfer function matrices have to satisfy for proper disturbance rejection. It should be noticed that the outputs have been scaled such that we require at each frequency $\|y(j\omega)\|_2 \leq 1$. Consequently, at frequencies where $\bar{\sigma}\{G_d\}$ is large we need a large control action for proper disturbance rejection (see Eq. 8). Typically, $\bar{\sigma}\{G_d\}$ is greater than one at low frequencies and drops to zero at high frequencies. Then, the frequency ω_d where the singular value of G_d crosses one is a useful controllability measure. This frequency is the minimum bandwidth requirement for feedback control. *A controller must be designed to produce a value of $\bar{\sigma}\{W_y S\}$ small in the range of frequencies lower than ω_d.* However, the control action may grow over its admissible limit, hence, to retain this value bounded, it is also necessary to consider the transfer function of Eq. 6. The disturbance rejection problem with bounded control action can then be defined in terms of the following transfer function matrix:

$$\begin{bmatrix} y \\ u \end{bmatrix} = \begin{bmatrix} W_y S G_d \\ W_u K S G_d \end{bmatrix} d = \begin{bmatrix} S_d \\ B_d \end{bmatrix} d = Md. \quad (10)$$

In the following we will consider disturbance signals with bounded energy, that is, $\|d(j\omega)\|_2 < \infty$. Then it is possible to write a necessary and sufficient condition for disturbance rejection in terms of the structured singular value (Doyle et al., 1982), introducing two virtual uncertainty blocks in the loop as is shown in Figure 1b where $\Delta_d \in \Pi$ and $\Delta_b \in \Pi$ and

$$\Pi = \{\Delta \mid \bar{\sigma}\{\Delta\} \leq 1\}.$$

Then the necessary and sufficient condition for disturbance rejection with bounded control energy is as follows:

Theorem 1. The closed-loop system has disturbance rejection capabilities with limited control action if, and only if, the structured singular value $\{\mu[M(j\omega)]\}$ is smaller than one for all frequencies.

Proof. It is straightforward from Doyle et al., 1982.

Francis (1984) proposes the minimization of the $\|M(s)\|_\infty$ in order to obtain minimum energy in $y(j\omega)$ and $u(j\omega)$. However, it is known that this solution is conservative. To obtain a controller that minimizes the energy of $y(j\omega)$ and $u(j\omega)$ we must solve the minimization of $\|\mu[M(s)]\|_\infty$, but this is a problem without solution at the moment. A suboptimal solution can be obtained using a $K-D$ interaction as proposed by Doyle (1985). All these alternatives require sophisticated computing algorithms and usually give rise to very high order controllers.

In the next section we will propose a methodology to adjust the structured singular value of the M matrix to a desired value by shaping the individual singular values of each block. In this form, if we adjust the structured singular value of an M matrix as a function of frequency, then the system will reject the disturbance in the frequency range of interest while the control action remains lower than a prespecified value.

Loop-Shaping Methodology

Loop-shaping mechanism

From the last section, it is clear that if $\mu(M)$ is less than one for all frequencies, then the closed-loop system satisfies the disturbance rejection specifications with limited control action. Freudenberg (1989) proposed some bounds over the μ value, as a function of the maximum singular value of the different blocks of M. In our case, these bounds can be defined as

$$\mu(M) \geq (\bar{\sigma}\{S_d\}\bar{\sigma}\{B_d\})^{1/2} - \max(\bar{\sigma}\{S_d\}, \bar{\sigma}\{B_d\}) \quad (11)$$

$$\mu(M) \leq (\bar{\sigma}\{S_d\}\bar{\sigma}\{B_d\})^{1/2} + \max(\bar{\sigma}\{S_d\}, \bar{\sigma}\{B_d\}). \quad (12)$$

Equation 12 suggests the dependence of μ with the singular values of each block that forms the M matrix in Eq. 10. Then we can adjust the value of μ by manipulating the singular values

$$\bar{\sigma}\{S_d\}$$
$$\bar{\sigma}\{B_d\}. \quad (13)$$

Singular value decomposition (SVD) will be reviewed below within the context of perturbation theory. The ultimate goal will be to quantify how variations in a given system matrix (controller) affect the singular values of S_d and B_d. To simplify the notation, we consider only identity weighting matrices $W_u = W_y = I$.

The following theorem and its corollary establish the relationships between a perturbed matrix and the nominal one (Agamennoni et al., 1988, 1992).

Theorem 2. Let $A, A' \in \mathbb{C}^{n \times n}$, and define the perturbed matrix as

$$A' = A(I + \Psi)$$

with

$$\Psi = V \Phi V^H,$$

where $V = [v, \ldots, v_n]$ and $W = [w_1, \ldots, w_n]$ are the eigenvector matrices of $A^H A$ and $A'^H A'$, respectively, and $\Phi \in \mathbb{C}^{n \times n}$. Note that V and W are unitary matrices. Furthermore, define

$$G = (D_\sigma)^{1/2}(I + \Phi)$$

with

$$D_\sigma = \text{diag}\{\sigma_k^2\{A\}\} = V^H A^H A V.$$

Then,

$$w_k = V\gamma_k,$$

where γ_k is the kth column-eigenvector of $G^H G$.

Corollary 1. If Φ is a diagonal matrix,

$$\Phi = \text{diag}\{\alpha_k\},$$

where $\alpha_k \in \mathbb{C}$, then the singular values of A' can be expressed as

$$\sigma_k\{A'\} = \sigma_k\{A\}|1 + \alpha_k|, \quad k = 1,2,\ldots,n.$$

Furthermore,

$$w_k = v_k,$$

that is, the eigenvectors of $A'^H A'$ are the same as those of $A^H A$.

For the proofs of this theorem and its corollary see Agamennoni et al. (1992). These results are significant since they allow the formulation of simple relationships between singular values and singular vectors of a perturbed matrix with respect to the nominal one.

Shaping the singular values of S_d

In this section we apply the results of Theorem 2 to the specific problem of adjusting the singular values of the disturbance sensitivity (DS) matrix, that is, shaping the frequency-dependent singular values of the matrix

$$S_d = (I + GK)^{-1} G_d.$$

This is equivalent to adjusting the singular values of the disturbance return difference (DRD) matrix

$$F_d = G_d^{-1}(I + GK).$$

Note that we have used the names disturbance sensitivity and disturbance return difference to differentiate these matrices from the analogous matrices without disturbance transfer function G_d. The shaping of the singular values of the DRD matrix will be performed by perturbing the controller matrix.

Let K be an original stable controller and define a new (perturbed controller) K' as follows:

$$K' = K + \Delta_K.$$

Accordingly, the perturbed DRD matrix F_d' is given by

$$F_d' = G_d^{-1}[I + G(K + \Delta_K)].$$

From Corollary 1, matrix F_d' can be expressed as

$$F_d' = G_d^{-1}(I + GK)(I + \Psi), \tag{14}$$

where $\Psi = V \Phi V^H$ and the columns of V are the eigenvectors of $F_d^H F_d$. Moreover, $\Phi = \text{diag}\{\alpha_k\}$ with a scalar complex variable α_k. Then, if the α_k are equal for all $k = 1, \ldots, n$, Δ_K is given by

$$\Delta_K = (G^{-1} + K)\Psi, \tag{15}$$

and the perturbed singular values of DRD are modified as follows

$$\sigma_k\{F_d'\} = |1 + \alpha_k| \sigma_k\{F_d\}.$$

Then, a properly evaluated set of α_k allows us to shape the desired singular values on a given frequency range.

Shaping the singular values of B_d

Now let us apply the results of Theorem 2 to the transfer function between the disturbance input to the control action, that is, shaping the frequency dependence of the singular values of the matrix

$$B_d = K(I + GK)^{-1} G_d.$$

Following similar steps as for the DS matrix, we conclude that if Δ_K is given by

$$\Delta_K = [I - GK(I + \Psi)]^{-1} K \Psi. \tag{16}$$

Then from Corollary 1, the perturbed matrix B_d' can be expressed as

$$B_d = K(I + GK)^{-1} G_d (I + \Psi), \tag{17}$$

and the perturbed singular values are modified as follows

$$\sigma_k\{B_d'\} = |1 + \alpha_k| \sigma_k\{B_d\}.$$

Hence, as before, a properly evaluated set of α_k allows us to shape the desired singular values on the given frequency range.

Equation 11 suggests that the structured singular value for this problem depends mainly on the singular values of S_d and B_d. Moreover, Eqs. 15 and 16 give the necessary perturbations needed on the original controller to achieve the shaping of the singular values of these matrices, which in turn will produce the desired shaping of the structured singular values. Equations 15 and 16 also give a parameterization of the singular values of nominal and perturbed S_d and B_d in terms of the α-functions.

The next proposition deals with the closed-loop stability of the perturbed system.

Proposition 1. Assuming the stability of the nominal system, then the perturbed (adjusted) system will be stable if:

(a) $\Psi + I$ has no zeros in the right half-plane (for shaping of the singular values of S_d), or

(b) Ψ has no poles in the right half-plane (for shaping of the singular values of B_d)

Proof. It is straightforward from Eqs. 14 and 17.

From these results the following user interactive algorithm can be devised to design controllers with disturbance rejection specifications and bounds over the control action.

Algorithm

Data. The pair of weighting functions W_u and W_y, an initial controller K_0, and a positive real number $\gamma_0 \leq 1$.

Step 0. Set $i = 0$.

Step 1. For controller K_i compute

$$\overline{S_d} = \max_\omega \bar{\sigma}\{S_d(j\omega)\}$$

and

$$\overline{B_d} = \max_\omega \bar{\sigma}\{B_d(j\omega)\}.$$

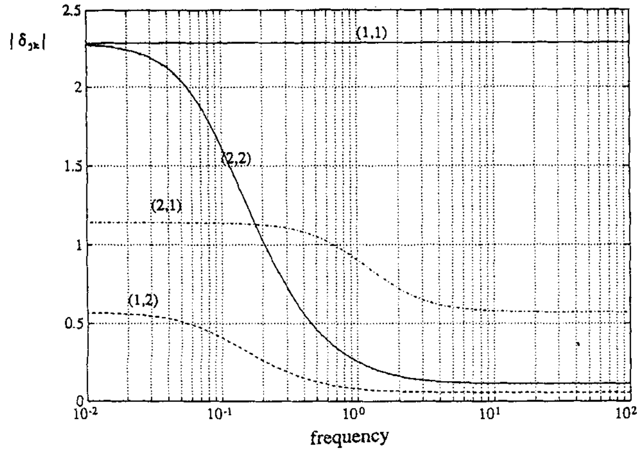

Figure 2. Modulus of δ_{ij} as function of the frequency.

Step 2. If $\max\{\bar{S}_d, \bar{B}_d\} \le \gamma_i$ go to step 3. Otherwise, if $\{\bar{S}_d > B_d\}$ select an α-function such that $\bar{\sigma}\{S_d(\omega)\}\{I + \alpha(\omega)\} < \gamma_i$ and compute K_{i+1} using Eq. 15. Set $i = i+1$ and return to Step 1. Otherwise, select an α-function such that $\bar{\sigma}\{B_d(\omega)\}\{I + \alpha(\omega)\} < \gamma_i$ and compute K_{i+1} using Eq. 16. Set $i = i+1$ and return to Step 1.

Step 3. If $\mu[M(s)] \le 1$, stop. Otherwise, choose $\gamma_{i+1} < \gamma_i$, and return to step 0.

The following remarks are in order:

Remark 1. A close examination of this algorithm shows that it may break down in step 2, whenever an α-function could not be found to produce $\max\{\bar{S}_d, \bar{B}_d\} \le \gamma_i$. In this case, a possible option is to relax the design specifications given by the weighting functions W_u and W_y. This is because of the classic trade-off between disturbance rejection and limited control action. Obviously, if we define only one requirement, the trade-off does not exist and the design of the controller is straightforward and no iterations are required.

Remark 2. It is obvious that each iteration of this algorithm adds to the new controller additional dynamics. The idea of returning to step 0 from step 3 is to reduce the additional dynamics if the original choice of γ is too large.

Remark 3. It is important to notice that the controllers of Eqs. 15 and 16 can result in expressions not physically realizable. However, we can always find a realizable approximation of these compensators, over any given finite frequency range.

Remark 4. The use of a single α-function is an alternative suitable for our case, because in this way we are modifying all the singular values in the same magnitude. This choice makes the evaluation of the new controller simpler, since $\psi = \alpha$.

The evaluation of this α-function can be performed easily in a graphical interactive environment. In our implementation we used the "drawmag" function from the μ synthesis toolbox (Balas et al., 1991) to create a stable minimum phase function from a given set of points selected from a graph with the assistance of a pointer device.

Examples

The methodology discussed earlier will now be tested within the context of two examples. The first one is rather simple because it is intended to clearly illustrate the proposed loop-shaping procedure. The second example is an existing industrial (C_3-splitter) column strongly affected by sluggish disturbances in the feed and in the cooling system of the condenser.

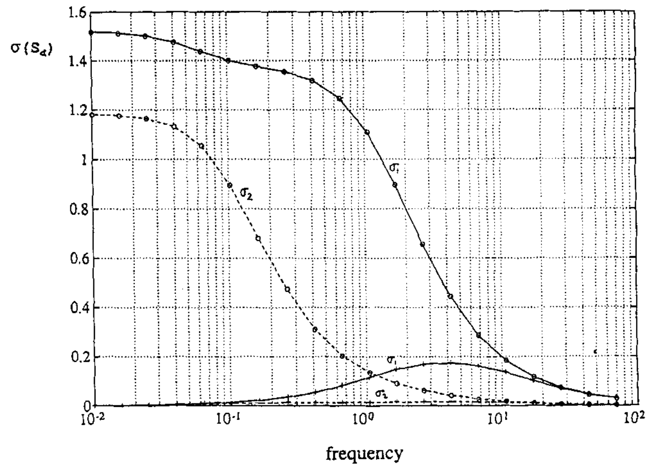

Figure 3. Frequency response of $\bar{\sigma}\{S_d\}$.

-o-o-o-o- Before compensation; - + - + - + - + - after compensation.

Example 1 (Simple Example). Let a plant model be described by the following transfer function matrices:

$$G = \begin{bmatrix} \dfrac{1}{s+1} & \dfrac{0.5}{s+2} \\ \dfrac{0.5}{s+1} & \dfrac{2}{s+2} \end{bmatrix}$$

$$G_d = \begin{bmatrix} \dfrac{2}{s+1} & 0 \\ 0 & \dfrac{2}{10s+1} \end{bmatrix}.$$

In this example the weighting matrices are $W_u = W_y = I$ (both output signals have the same order of magnitude). Figure 2 shows the modulus of δ_{jk} for $j,k = 1,2$. Analysis of this figure suggests that when disturbance 1 enters the system the manipulated control action 1 should be larger than the manipulated control action 2. With respect to the effect of disturbance 2, the manipulated control action 2 should be larger than the manipulated control action 1, though in this case in a more narrow frequency band.

A diagonal matrix with gain of 0.5, that is, $K = 0.5I$ was considered as the initial controller. Figure 3 shows the singular values of the disturbance sensitivity function for the original controller. We can see that the magnitude of the maximum singular value is larger than one at low frequencies (≈ 1.5), while it falls off at higher frequencies (lower than 0.2 for frequency 10 and over). This implies that $\bar{\sigma}(F_d)$ is lower than one at low frequencies. Then, the function $(1+\alpha)$ must be larger in low frequencies and drops to zero at high frequencies, in order to increase the value of $\bar{\sigma}(F_d)$ in the necessary frequency region. Then, we choose an α-function as

$$\alpha = \frac{s+10}{s} - 1.$$

Figure 3 also shows the resulting singular values. Here we can see that the maximum singular value is lower than 0.2.

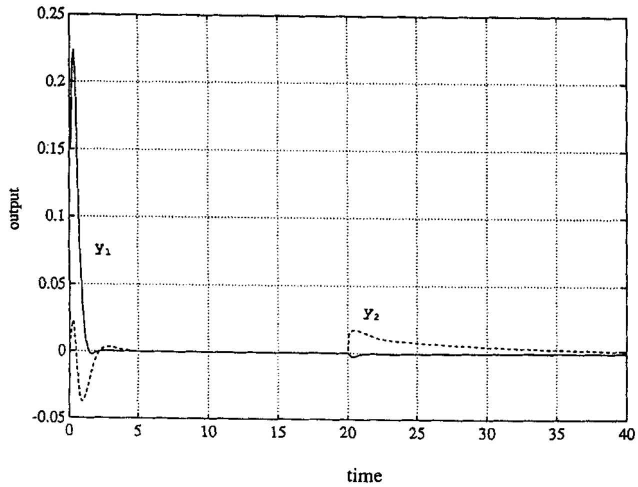

Figure 4. Time simulation of the output variables.

Figure 4 shows the time response of the system outputs for the resulting closed-loop system when a unitary step change in disturbance 1 is applied to the system at time $t = 0$, and in disturbance 2 at time $t = 20$. We can see different behavior due mainly to the difference in the numerical values of the time constants of G_d. Clearly, when a step change in d_1 is applied [the time constant of $G_d(1,1)$ is 1] the effect in the output is larger and faster than if we had applied the step change in d_2 [the time constant of G_d (2, 2) is 10].

Example 2. Consider now the problem of controlling a (C_3-splitter) distillation column. This is actually an existing column, and an input–output model is available from rigorous simulation (using Speed-up) and plant trials. Both the process transfer function and the disturbance transfer function are as follows. (The process has very large time constants, and small dead time were observed (compared with the time constant of the system) in the real plant. Thus, dead times were not considered here; however, this is not a restriction for this methodology and they were incorporated in posterior calculation, but no significant effect was observed.)

$$G = \begin{bmatrix} \dfrac{0.01}{550s+1} & \left(\dfrac{1.24}{38.5s+1} - \dfrac{6.32}{1290s+1}\right)10^{-3} \\ 0 & \dfrac{58.}{85s+1} \end{bmatrix}$$

$$G_d = \begin{bmatrix} \dfrac{-0.23}{550s+1} & \dfrac{0.0003}{240s+1} \\ 0 & \dfrac{23.3}{240s+1} \end{bmatrix},$$

where the propane impurity in the distillate (XD_3) and the top pressure (P) are the controlled variables (y_1 and y_2 respectively), and the distillate flowrate (D) and the heat input to the reboiler (Q_{REB}) are the manipulated variables (u_1 and u_2). The disturbances d_1 and d_2 are the feed composition (X_F) and the ambient air wet-bulb temperature (T_{wb}).

Typical disturbance inputs are steps of magnitude 0.0015 mol fraction for the feed composition and 8°C for wet-bulb temperature. Here, due to physical and production requirements, the variations on the output signals have constraints of a different order of magnitude. The propane impurity must be less than 8×10^{-3} mole fraction, while the pressure must be less than 1,500 kPa. Consequently, the weighting function matrix is chosen as

$$W_y = \begin{bmatrix} 1{,}000 & 0 \\ 0 & 1 \end{bmatrix}.$$

In the case of the manipulated variables, the distillate flowrate must be bounded by 2.5 kmol/min and 5.5 kmol/min as lower and upper bounds, and the heat input to the reboiler must be less than 20 MJ/s. The weighting function matrix is then $W_u = I$. The first design objective in this column is then to keep both the controlled and the manipulated variables within these limits in the presence of disturbances.

As a first step of the design, we will consider only the loop-shaping of the maximum singular value of the weighting sensitivity matrix.

The original controller was taken to be a diagonal matrix with gain of 0.1, that is, $K = 0.1I$. Figure 5a shows the singular values of the disturbance sensitivity function for this initial controller. It can be seen that the magnitude of the maximum singular value is larger than one for a large frequency range. Then the alpha functions must shape this singular value to fall below one at this frequency range. This is equivalent to shaping the singular values of F_d to be larger than one for all frequencies. This can be achieved by choosing the α-functions as

$$\alpha = \frac{6s+1}{s} - 1.$$

Figure 5b shows the singular values of the closed-loop system with the new controller. Here we can see that the maximum singular value of the sensitivity matrix is less than 0.55 at the critical frequency of 0.1. Figure 6 show the plot of $\bar{\sigma}\{KSG_d\}$ as a function of the frequency. It is clear that the control action exceeds the permissible bounds. Figures 7a and 7b shows the system outputs XD_3 and P, respectively, when a step change is applied in feed composition and wet-bulb temperature. From this figure, we can appreciate the disturbance rejection capabilities of the new controller. Figures 8a and 8b, on the other hand, show the values for the corresponding manipulated variables. In this case, the amplitude of the distillate flowrate exceeds the maximum permissible bound. Also, we can see that the amplitude of both control variables is larger when wet-bulb temperature disturbance is applied than when feed composition disturbance is applied.

Now, we will consider the problem of disturbance rejection with bounded control energy, that is, adjusting the μ-function of the two blocks M matrix. The original controller was taken to be $K = 0.005I$. Figures 9a and 9b show the plots of $\bar{\sigma}\{W_y SG_d\}$ and $\bar{\sigma}\{KSG_d\}$ as a function of the frequency for the initial controller. It can be seen that the magnitude of $\bar{\sigma}\{W_y SG_d\}$ is larger than one for a large frequency range, while the magnitude of $\bar{\sigma}\{KSG_d\}$ is very small. The major contribution to μ is due to the singular value of the weighted sensitivity matrix. Then the alpha functions must shape $\bar{\sigma}\{W_y SG_d\}$ to fall below one at this frequency range. This was achieved by choosing α as

$$\alpha = \frac{1.104s^2 + 2.0667s + 1}{1.2362s^2 + 0.0316s},$$

and it is applied to Eq. 15 to compute the new controller. Figure 10 shows the singular values for this controller. Here we can see that these values are lower than one in the frequency range of interest. Figure 11 shows the value of μ, as measures of disturbance rejection and limited control action, as a function of the frequency. From this plot it is clear that μ is lower than one for all frequencies. Thus the new controller satisfies the joint specifications of disturbance rejection with bounded control signal.

Figures 12a and 12b shows the system outputs XD_3 and P, respectively, when a step change is applied in feed composition and wet-bulb temperature. From these figures, we can appreciate the disturbance rejection capabilities of the new controller. Figures 13a and 13b shows the values for the corresponding manipulated variables. Now the magnitude of these variables is lower than the specified bounds.

To compare the results, we also considered a controller designed by minimizing the H_∞-norm of the M matrix. After 5 $K-D$ iterations of the μ design, a controller was found

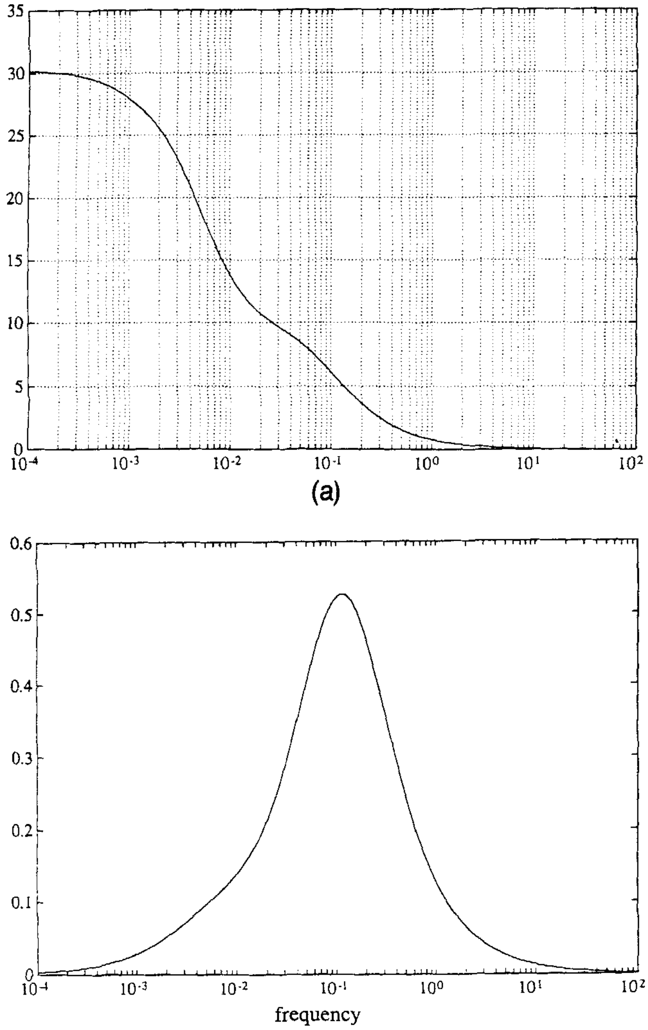

(a) (b)

Figure 5. (a) Frequency response of $\bar{\sigma}\{S_d\}$ for the initial controller; (b) frequency response of $\bar{\sigma}\{S_d\}$ for the adjusted controller.

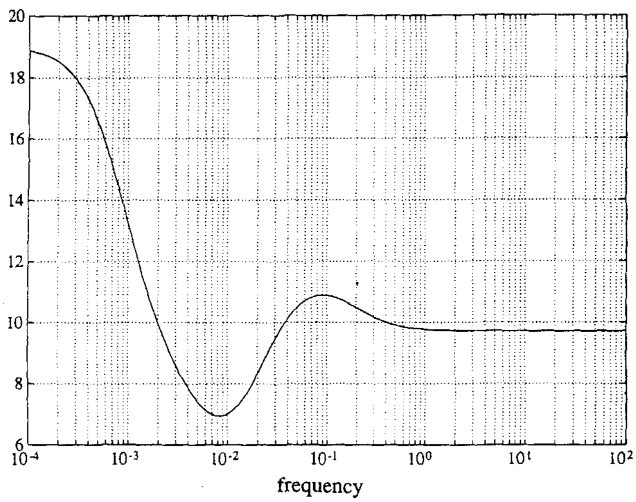

Figure 6. Frequency response of $\bar{\sigma}\{KSG_d\}$ for the adjusted controller.

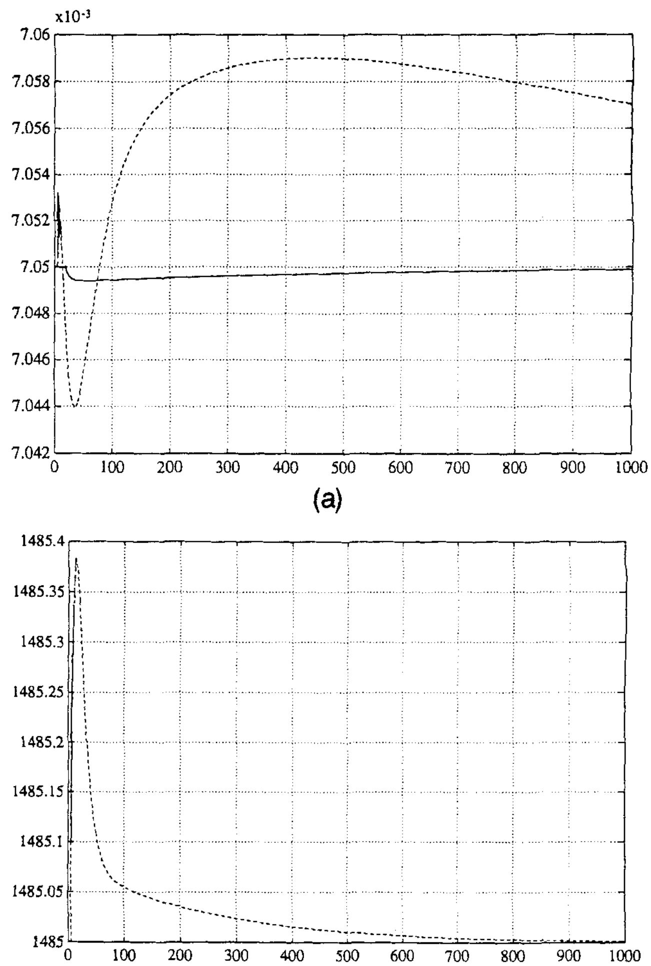

(a) (b)

Figure 7. (a) Time simulation of the XD_3; (b) time simulation of the pressure.

—— Step in X_F; ------ step in T_{wb}.

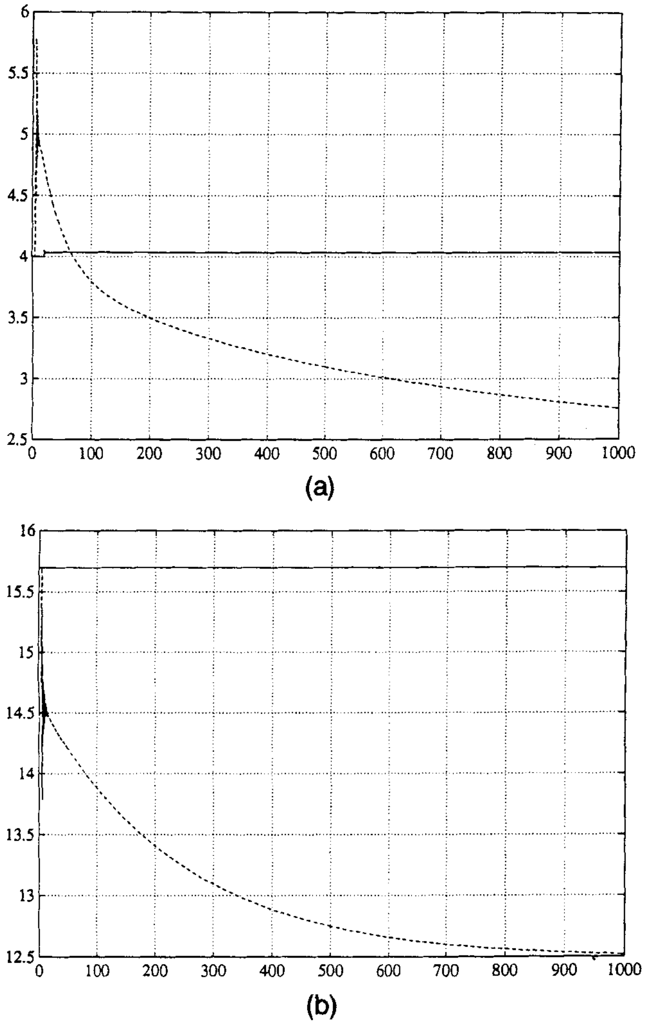

Figure 8. (a) Time simulation of the *D*; (b) time simulation of the Q_{REB}.

—— Step in X_F; ------ step in T_{wb}.

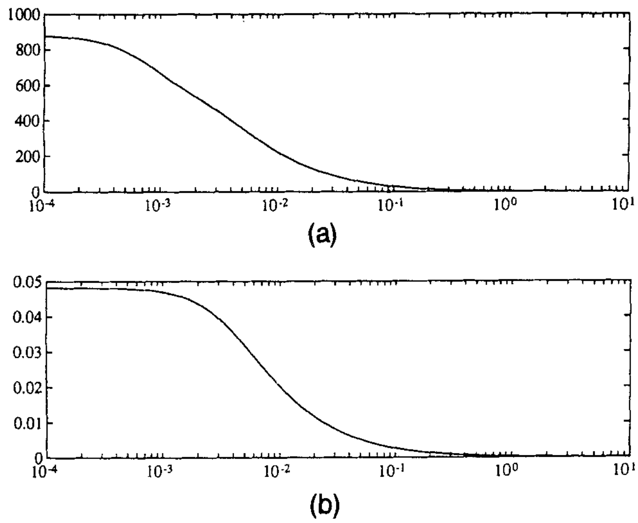

Figure 9. (a) Frequency response of $\bar{\sigma}\{W_y SG_d\}$ for the initial controller; (b) frequency response of $\bar{\sigma}\{KSG_d\}$ for the initial controller.

that satisfies the joint specifications of disturbance rejection and bounded control energy (Balas et al., 1991). Figure 14 shows the plot of μ as function of the frequency for each $K-D$ iteration (the case "it.1" is the H_∞ controller). These values are lower than the values obtained using the loop-shaping methodology. However, in this case the controller order is 55 against the fourth-order compensator computed using our technique.

Figures 15a and 15b show the system outputs XD_3 and P, respectively, when a step change is applied in the feed composition and wet-bulb temperature for the H_∞ controller. The values for the corresponding manipulated variables are also shown in Figures 16a and 16b. The equivalent plots for the fifth iteration controller are in Figures 17 and 18.

From these figures it can be seen that the resulting high-order controller has better disturbance rejection capabilities in comparison to the loop-shaping controller. However, the high order of the resulting controllers makes the immediate

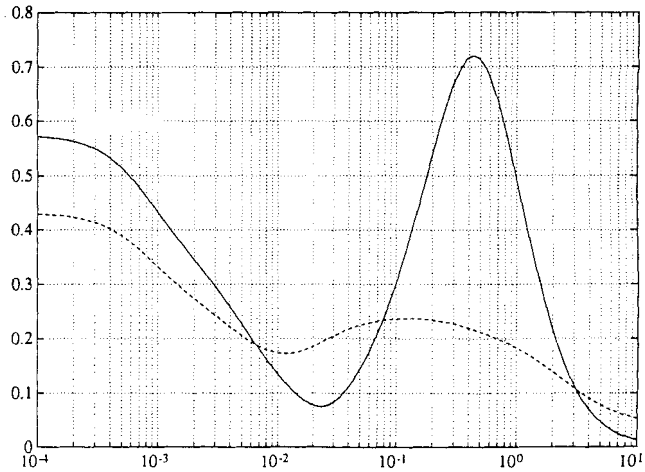

Figure 10. Frequency response for the adjusted controller.

$\bar{\sigma}\{W_y SG_d\}$ (——); $\bar{\sigma}\{KSG_d\}$ (----).

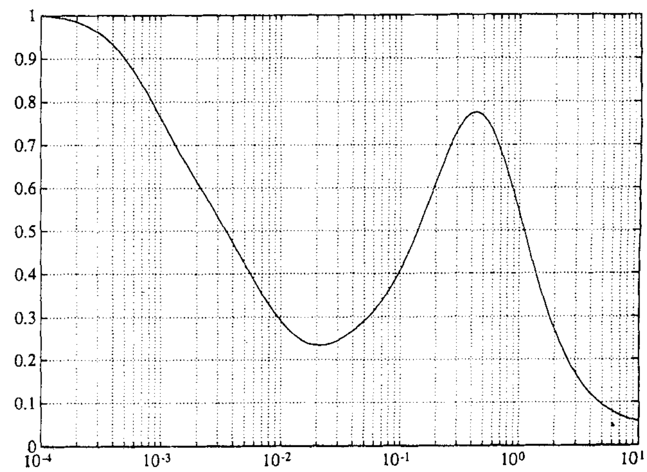

Figure 11. Frequency response of μ for the adjusted controller.

application very difficult in comparison with the low-order controller obtained with the technique proposed in this article. Of course, we can always apply some reduction order technique to obtain a reduced version of the $D-K$ iteration controller. However, after the reduction of the $D-K$ iteration controller there is no guarantee that the resulting low-order controller will maintain the original performance. It is possible that the reduced controller will have similar behavior to that of the loop-shaping designed controller.

Conclusions

The suppression of the impact that disturbances have on the operating behavior of processing units was addressed. First, the discussion centered on the different characteristics between plants that have disturbance transfer matrices with small and large bandwidth and the effect of having disturbances with components of low and/or high frequencies. Then a methodology to design controllers with disturbance rejection capabilities and bounds over the manipulated variables

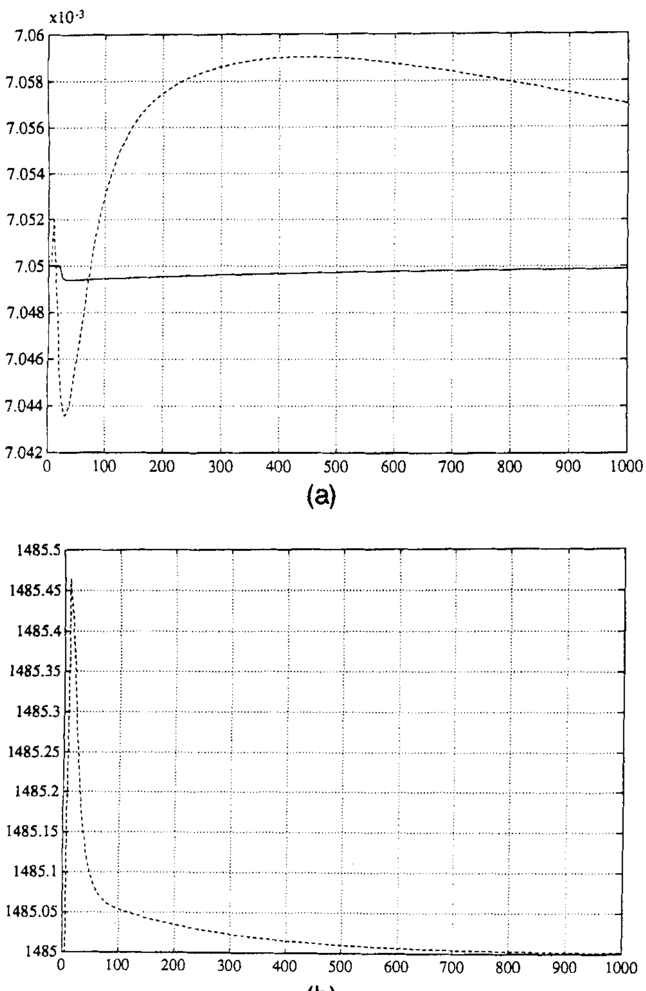

Figure 12. (a) Time simulation of the XD_3 for loop-shaping controller; (b) time simulation of the pressure for loop-shaping controller.
—— Step in X_F; ------ step in T_{wb}.

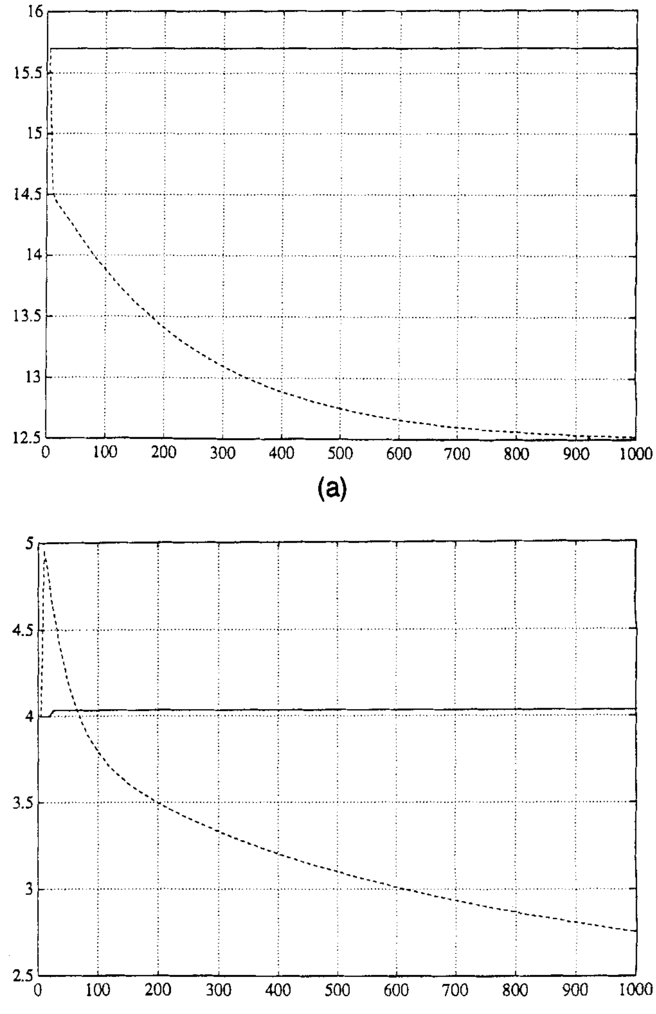

Figure 13. (a) Time simulation of the D for loopshaping controller; (b) time simulation of the Q_{REB} for loop-shaping controller.
—— Step in X_F; ------ step in T_{wb}.

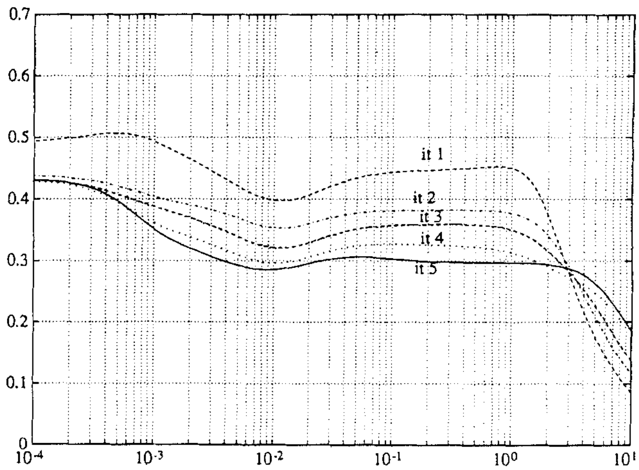

Figure 14. Frequency response of μ for each $D-K$ iteration.

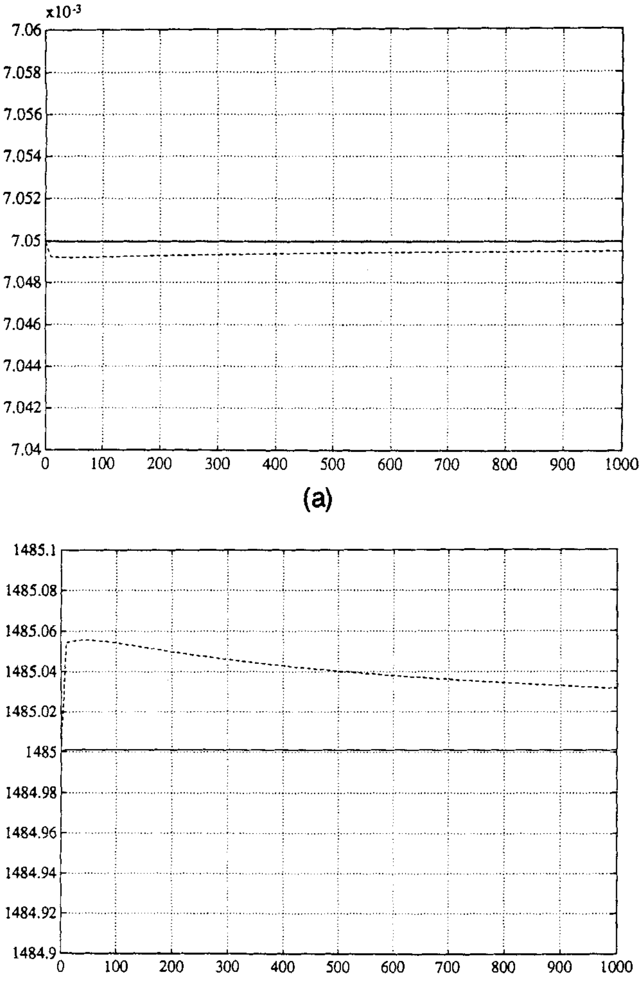

Figure 15. (a) Time simulation of the XD_3 for H_∞ controller; (b) time simulation of the pressure for H_∞ controller.

—— Step in X_F; ------ step in T_{wb}.

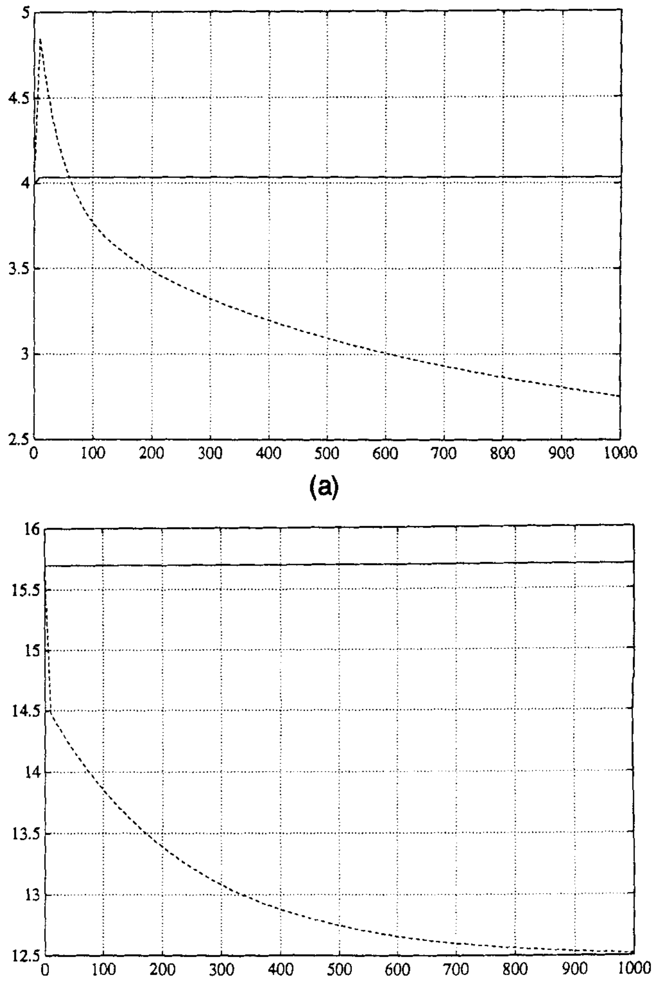

Figure 16. (a) Time simulation of the D for H_∞ controller; (b) time simulation of the Q_{REB} for H_∞ controller.

—— Step in X_F; ------ step in T_{wb}.

was presented. We based our developments in the shaping of each component with contribution in the final value of the μ-function of a given closed-loop matrix. This approach allows us to establish a general framework to the solution of the general disturbance rejection problem. The usefulness of this technique was finally discussed within the context of two examples, one of them an existing distillation column.

Notation

B_d = weighting transfer matrix from $d(s)$ to $u(s)$
S_d = disturbance sensitivity matrix

Literature Cited

Agamennoni, O. E., A. C. Desages, and J. A. Romagnoli, "Robust Controller Design Methodology for Multivariable Chemical Processes," *Chem. Eng. Sci.*, **43**(11), 2937 (1988).

Agamennoni, O. E., J. L. Figueroa, G. W. Barton, and J. A. Romagnoli, "Advanced Control Design for a Distillation Column," *Int. J. Contr.*, **59**(3), 817 (1994).

Agamennoni, O. E., J. L. Figueroa, A. C. Desages, J. A. Romagnoli, and A. Palazoglu, "A Generalised Loop-Shaping Technique for Design of Multivariable Feedback Control Systems," *Proc. Amer. Contr. Conf.*, p. 896 (1992).

Balas, G., J. Doyle, K. Glover, A. Packard, and R. Smith, *μ-Analysis and Synthesis Toolbox. MATLAB Functions for the Analysis and Design of Robust Control Systems*, MySyn Inc. and The Math Works Inc. (1991).

Chang, B., and J. Pearson, "Optimal Disturbance Reduction in Linear Multivariable Systems," *IEEE Trans. Automat. Contr.*, **AC-29**(10), 880 (1984).

Doyle, J., "Analysis of Feedback Systems with Structured Uncertainty," *IEE Proc., Part D*, **129**(6), 242 (1982).

Doyle, J., J. Wall, and G. Stein, "Performance and Robustness Analysis for Structured Uncertainty," *Proc. Conf. on Decision and Control*, Orlando, FL, p. 629 (1982).

Doyle, J., "Structured Uncertainty in Control System Design," *Proc. Conf. on Decision and Control*, Ft. Lauderdale, FL, p. 260 (1985).

Francis, B., and G. Zames, "On H_∞-Optimal Sensitivity Theory for SISO Feedback Systems," *IEEE Trans. Automat. Contr.*, **AC-29**(1), 9 (1984).

Francis, B., "Optimal Disturbance Attenuation with Control Weighting," in *Systems and Optimization, Proceedings of the Twentieth Workshop, Enschode, The Netherlands*, Lectures notes in Control and Information Sciences, Springer-Verlag, New York, p. 98 (1984).

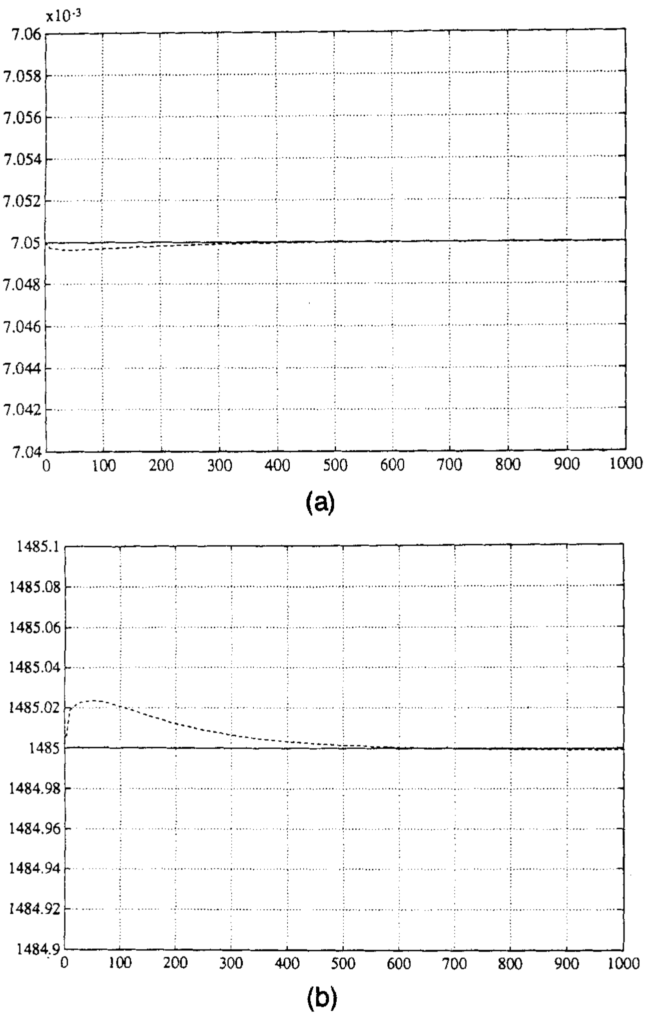

Figure 17. (a) Time simulation of the XD_3 for 5th $D-K$ iteration controller; (b) time simulation of the pressure for 5th $D-K$ iteration controller.

—— Step in X_F; ------ step in T_{wb}.

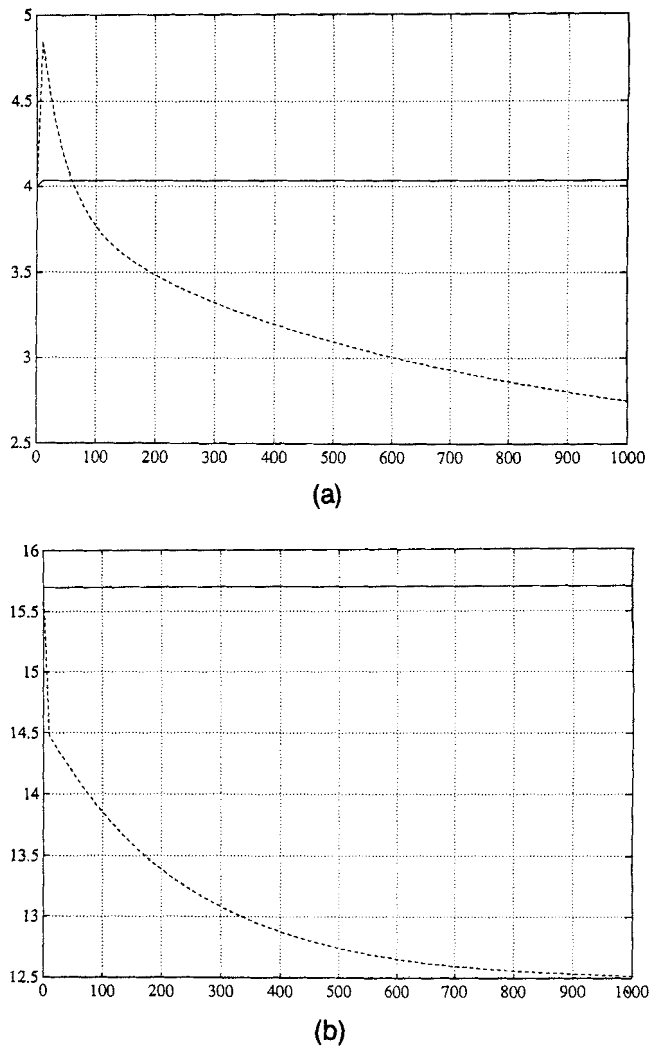

Figure 18. (a) Time simulation of the D for 5th $D-K$ iteration controller; (b) time simulation of the Q_{REB} for 5th $D-K$ iteration controller.

—— Step in X_F; ------ step in T_{wb}.

Freudenberg, J., "Analysis and Design for Ill-Conditioned Plants. Part 1. Lower Bounds on the Structured Singular Values," *Int. J. Contr.*, **49**(3), 851 (1989).

McCune, L. C., and P. W. Gallier, "Digital Simulation: A Tool for the Analysis and Design of Distillation Controls," *ISA Trans.*, **12**, 193 (1973).

Skogestad, S., and E. Wolff, "Controllability Measures for Disturbance Rejection," paper presented at the IFAC Workshop on Interactions between Design and Process Control, Imperial College, London (Sept. 6–8, 1992).

Wolff, E., S. Skogestad, M. Hovd, and K. W. Mathisen, "A Procedure for Controllability Analysis," paper presented at the IFAC Workshop on Interactions between Design and Process Control, Imperial College, London (Sept. 6–8, 1992).

Zames, G., and B. Francis, "Feedback, Minimax Sensitivity, and Optimal Robustness," *IEEE Trans. Automat. Contr.*, **AC-28**(5), 585 (1983).

Manuscript received Sept. 20, 1993, and revision received Dec. 12, 1994.